Future Network and MobileSummit 2011 Conference Proceedings
Paul Cunningham and Miriam Cunningham (Eds)
IIMC International Information Management Corporation, 2011
ISBN: 978-1-905824-25-0

Adaptive Downlink Power Control for HSDPA Femtocells

Massinissa Lalam[1], Ioannis Papathanasiou[2], Masood Maqbool[1], Thierry Lestable[3]
[1]*SAGEMCOM E&T,* [3]*SAGEMCOM SAS, 250 Route de l'Empereur, Rueil-Malmaison, 92500, France*
[2]*EURECOM, 2229 Route des Crêtes, Sophia-Antipolis, 06560, France*
Email:massinissa.lalam@sagemcom.com

Abstract: Femtocell is emerging as a key technology to improve both the coverage and the capacity in indoor environments, whilst enabling innovative services. Since co-channel deployment of the femtocell network over the existing macrocell one is the most commercially viable solution, a closed/hybrid access policy may lead to severe co-channel interference problems. Therefore, the femtocells have to be carefully operated to disturb as less as possible the macrocell users whilst offering higher throughput to femtocell consumers. In this paper, we propose a dynamic downlink power control mechanism for femtocells, based on the Channel Quality Indicator (CQI) reports. Our results demonstrate that this provide an effective balance between femto users' throughput and femtocell impact on the macrocell performance without modifying the existing back-haul requirements.

Keywords: HSDPA, CQI, femtocells, adaptive power control

1. Introduction

According to the Femto Forum [1], an industry consortium which promotes femtocells, femtocells are low-power (100mW or less), small-form and very low-cost cellular base stations (thus operating in licensed spectrum) designed to be user-deployed within indoor environments such as houses, malls or offices. A femtocell is connected to the macrocell network via a broadband internet connection, e.g. an Internet Protocol (IP) network over an existing x Digital Subscriber Line (xDSL). Recently, the 3rd Generation Partnership Project (3GPP) has standardised Universal Mobile Telecommunication System (UMTS) / Long Term Evolution (LTE) femtocells [2]. While LTE is a rapidly growing technology, UMTS supporting High Speed Packet Access (HSPA) in uplink (HSUPA) and downlink (HSDPA) still benefits from deployment increase worldwide [3]. With first commercial release of femtocells being HSPA, the interest on 3G femtocell has never been so strong, thus our focus on FDD HSDPA in this paper.

Despite the self-evident benefits for a femtocell owner in terms of transmission quality, there are many technical challenges to cope with femtocell deployment. Due to their large numbers and their arbitrary location, the interference mitigation becomes a challenging task. Femto Forum has published a number of white-papers that describe extensively this issue for UMTS/LTE systems [1, 4]. Among the addressed scenarios, the most critical one is the downlink co-channel (same carrier) deployment with femtocells in closed access. In such mode a femtocell denies the use of network through it to all users not belonging to its Closed Subscriber Group (CSG). If no action is taken, a Macrocell User Equipment (MUE) not in the femtocell CSG will be highly interfered in the vicinity of the femtocell and could even lose its network connection. In order to minimise the deployment cost and enable simple plug-and-play devices that can coexist

with the macro network, femtocells have to fully embrace leading edge self-configuration and self-optimisation techniques.

Several works exist in recent literature that deal with mitigating femtocell interference issues by adjusting the femtocell transmit power. Authors of [5] and [6] present a transmit power algorithm in which each 3G femtocell (called Home Node B (HNB) within 3GPP standard) adapts its transmission power in order to maintain a minimum quality level for the macrocell control channel (CPICH). This power setting is based on the received signal strength coming from the macro network and measured by the HNB. Such measurement can be facilitated thanks to a Network Listen Module (NLM) that enables the HNB to sniff its neighbouring environment like a normal UE would do. Similarly, [7] and [8] give a transmit power calculation formula taking into consideration the distance between the femtocell and the most powerful macrocell while maintaining a minimum coverage for its serving Home UE (HUE).

The main advantage of these "static" methods is the backward compatibility with the existing architecture since the power setting is performed autonomously by the femtocell using its NLM module. However, the femtocell may decrease its power while no MUE is in the vicinity, thus decreasing the HUEs' performance while it was not necessary. To detect the MUE presence, [9] proposes that the femtocell measures the uplink noise rise coming from the MUEs. In this way, the power adjustment may be triggered more wisely. One other drawback of an NLM-based power setting is that the measurements are made at the femtocell position and not at the victim MUE position. Some methods found in [10] propose that certain measurements carried out by the victim MUE are fed back to the femtocell meaning that new signalling and protected channels have to be introduced to convey such measurements. Such approach is beyond the scope of this paper.

While these NLM-based techniques are a good step toward the interference mitigation, there is a need for dynamic solutions that can deal with the interference while operating. Indeed, transmission is usually discontinued when NLM module is used to avoid the HNB to listen to its own emission. In this paper, we proposed a dynamic power control algorithm that exploits the feedback procedure in FDD HSDPA and the excellent transmission quality associated to a femtocell to adjust the downlink power transmission according to a given targeted QoS. The current QoS is directly deduced from the standardised feedback, thus no extra signalling (backward compatibility) nor extra measurement (from a UE or the NLM module) is required. The rest of the paper is organised as follows. Section 2. briefly recalls the HSDPA feedback reporting procedure. Section 3. presents the power control procedure. Section 4. describes the system model. Section 5. gives simulation results while Section 6. finally draws conclusions and identifies promising directions.

2. HSDPA

In HSDPA, two of the fundamental characteristics of UMTS, the variable spreading factor (SF) and the fast power control, were replaced by an adaptive modulation and coding (AMC), an extensive multi-code operation and a fast and spectrally efficient retransmission strategy. The use of more robust coding, fast HARQ and multi-code operation removed the need for variable SF which is now fixed and equal to 16. Instead of controlling the power of the UE, AMC selects through link adaptation a Modulation

and Coding Scheme (MCS) that reflects the UE channel condition. Indeed, the UE is able to feedback in the uplink High Speed Dedicated Physical Control Channel (HS-DPCCH) the downlink quality it perceived through the channel quality indicator (CQI) to its serving base station.

More precisely, the UE estimates the Signal to Interference-plus-Noise Ratio (SINR) it may experience on the High Speed Physical Downlink Shared Channel (HS-PDSCH). For this purpose, the UE derives the total received HS-PDSCH power $P_{\text{HS-PDSCH}}$ from the received power over the Common Pilot Channel (CPICH) P_{CPICH} according to:

$$P_{\text{HS-PDSCH}} = P_{\text{CPICH}} + \Gamma + \Delta \tag{1}$$

where powers are in dBm, Γ is a higher-layer configured offset and Δ is a power adjustment that depends on the UE category [11]. Usually, the CPICH power is equal to 10% of the total power, whilst 80% is dedicated to HS-PDSCH traffic.

The CQI indicates the highest MCS (transport block size, modulation type and number of parallel HS-PDSCH codes) that could be correctly received under such SINR in the downlink with a reasonable block error rate, usually around 10%. It is an integer ranging from 0 (UE in outage) to 30 (maximum throughput supported by the UE) for non configured MIMO UE [11]. In this paper we consider category 10 UEs, meaning that the maximum throughput they support is 14.4Mbps (15 HS-PDSCH codes with 16-QAM, $\Delta = 0$) [11].

The fast scheduler, located at the base station, uses this value (but not only) to determine to which terminal to transmit to and at which data rate. Table 1 gives a list of CQIs with their respective modulation schemes and achievable data rate. The CQIs were defined such that a 1dB increase of the transmission power allows the UE to support the next MCS, thus reporting CQI+1 instead of CQI [12].

Table 1: Some CQIs and their associated properties

CQI	**Mapping**	**#HS-PDSCH**	**Data Rate (Mbps)**
0	Out of Range		
1	QPSK	1	0.0685
12	QPSK	3	0.871
17	16-QAM	5	2.0945
22	16-QAM	5	3.584
30	16-QAM	15	12.779

3. Power control algorithm description

To perform scheduling, the Node B traditionally monitors the CQIs fed back by one UE in communication, which reflect the signal quality in the downlink. As shown by Table 1, each CQI has a maximum achievable data. To guarantee a given data rate to one HUE, the HNB could send him data with the corresponding MCS no matter what its reported CQI is (hard approach). Most likely, the transmitted MCS at TTI t will be:

$$\text{MCS}_t = \min(\text{CQI}, \text{MCS}_{\text{target}}) \tag{2}$$

We use here a different approach, where the HNB adjusts its downlink power such that the HUE reported CQI will meet the targeted one. Since CQIs have been designed

with 1dB resolution, if the reported CQI is one unit above/below the target, then 1dB decrease/increase in the transmission power will lead to a reported CQI equal to the target assuming no change in the channel conditions. The idea behind this approach is to exploit the low indoor user velocity (small channel variations) and the excellent transmission quality usually associated with a femtocell: even with low power transmission, a HUE can still report high CQI values (see Figure 3 for some usual HUE reported CQIs).

The goal of the dynamic power control described here is to maintain on average a target CQI ($\mathbf{CQI}_{\text{target}}$) for the HUE's reports. The HNB is keeping a monitoring window of length L during which it is supervising the consecutive reported CQI values. Since the last received CQI is more correlated to the upcoming one than the older CQIs, we define a normalised decreasing L-length filter via the column vector $\mathbf{W} = \{w_l\}_{0 \leq l < L}$ to weight the reported CQIs according to their time of arrival. We arbitrary allocate 60% of the weight to the last received CQI while the others share the 40% left in the following way:

$$\begin{cases} w_0 &= 0.6 \\ w_l &= 0.8 \dfrac{L-l}{L(L-1)} \quad 1 \leq l < L \end{cases} \tag{3}$$

Note that none of these coefficients is optimised, which is left for further studies.

Let $\mathbf{C}_t = \{c_{t-\tau l}\}_{0 \leq l < L}$ be the column vector collecting the L last reported CQIs, where t is the time of the last received CQI and τ represents the time window duration covering the CQI reporting period. We define the average CQI such as:

$$\overline{\mathbf{CQI}}_t = \mathbf{W}^{\mathrm{T}} \mathbf{C}_t = \sum_{l=0}^{L-1} w_l c_{t-\tau l} \tag{4}$$

When L consecutive CQI reports are above / below $\mathbf{CQI}_{\text{target}}$ at time t, the HNB adjusts, i.e. decreases or increases, correspondingly, its maximum transmit power according to the following equation in dBm:

$$P_t^{\mathrm{Tx}} = \min\left(P_{\max}, \max\left(P_{\min}, P_{t-1}^{\mathrm{Tx}} + \Delta_t\right)\right) \tag{5}$$

where $P_{\max}$ and $P_{\min}$ represent in dBm the maximum and minimum HNB transmit power, respectively. The power offset Δ_t to apply is easily computed as the difference between the targeted CQI and the average CQI:

$$\Delta_t = \begin{cases} \left\lfloor \mathbf{CQI}_{\text{target}} - \overline{\mathbf{CQI}}_t \right\rfloor & \text{if } \overline{\mathbf{CQI}}_t \leq \mathbf{CQI}_{\text{target}} \\ \left\lceil \mathbf{CQI}_{\text{target}} - \overline{\mathbf{CQI}}_t \right\rceil & \text{if } \overline{\mathbf{CQI}}_t > \mathbf{CQI}_{\text{target}} \end{cases} \tag{6}$$

where $\lfloor . \rfloor$ and $\lceil . \rceil$ denote the integer part and the smallest following integer, respectively. This distinction allows us to significantly increase the power when the average CQI is too low and to reasonably decrease the power when the average CQI is too high.

4. System Model

In order to evaluate accurately the above mentioned power control algorithm, an approach based on dynamic system-level simulation (SLS) is selected, thus allowing large-scale deployment performance assessment. We proceed through a classical Monte-Carlo

approach, where UEs and HNBs are randomly dropped over a 2D 3-sector 7-site hexagonal macrocell network at each run with the dual-stripes model (see Figure 1 and Figure 2). MUEs are randomly dropped in the entire 2D plan with a given percentage indoor, i.e. in one random block of a dual-stripes, while HUEs are randomly dropped in the block containing their serving HNB. The main system-level parameters are summarised in Table 2 and 3. For more details, the reader may refer to [13] for the macrocell layout and to [14] for the femtocell model (model 1 assumed for the propagation equations).

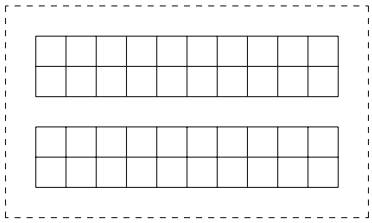

Figure 1: Dual-Stripes model

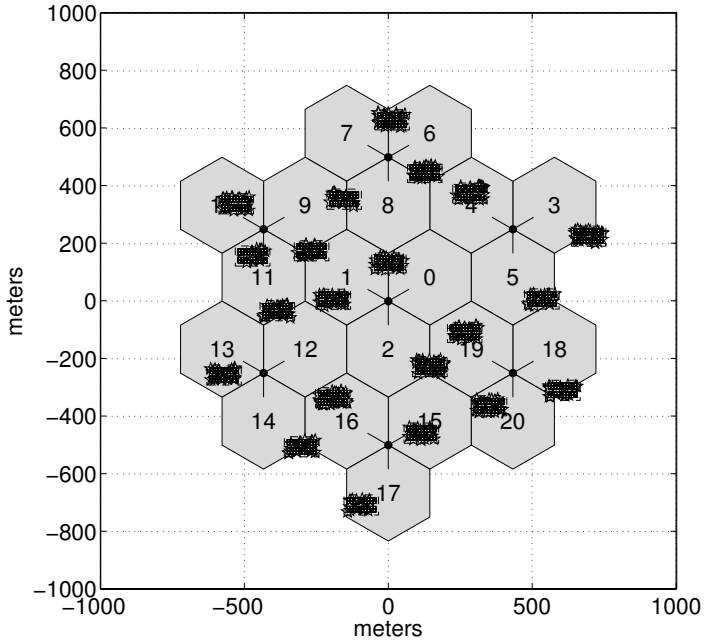

Figure 2: Macro and femto network, one drop example (top view)

One UE is attached to a base station according to the best long term received power which is equal in dB to the transmission power plus the antenna gain(s) minus the path-loss and the shadowing. All UEs have omni antenna gains (0dBi) and a noise figure of 9dB. A MUE is attached to its best Node B while a HUE is attached to the HNB located in the same block. Only the fast fading of the serving link is dynamically modelled using Rayleigh fading based on Jakes's multi-ray approach [15]. The ITU Pedestrian A power and delay profile is assumed with a user velocity of 3km/h. At the UE side, an ideal Rake receiver is considered [16].

All UEs have Full-Buffer traffic model. A UE reports its CQI every TTI, which will be processed by its serving base station at TTI + 3. Based on the last feedback, the base station uses proportional fair criteria to schedule its attached UEs every TTIs. We

Table 2: Macrocell layout

Parameter	**Value**
# Sites	7
# Sector per site	3
Site-to-Site distance	1000m
Tx power	43dBm
Antenna gain	cf. [14, Table A.2.1.1.2-2]
Pathloss	cf. [14, Table A.2.1.1.2-8]
Shadowing	8dB of standard deviation
# MUEs per sector	10 (35% indoor)

Table 3: Dual-Stripes model

Parameter	**Value**
# Clusters per sector	1 (uniform drop)
# Floors	6
# Blocks per stripe	20
Block size	10m $\times$ 10m
Exterior wall attenuation	20dB
Interior wall attenuation	5dB
HNB deployment ratio	10% (uniform drop)
Maximum Tx power	13dBm
Minimum Tx power	-23dBm
Antenna gain	0dBi (omni)
Pathloss	cf. [14, Table A.2.1.1.2-8]
Shadowing	4dB of standard deviation
# HUEs per HNB	1 (uniform drop in the block)

assume that a Node B can serve up to three UEs simultaneously at a given TTI, while the HNB will only serve one. Our platform also implements the HARQ mechanism configured with 4 processes and a maximum of 4 transmissions using Chase combining.

5. Results

5.1 One Drop Example

Figure 3 gives the repartition of the reported CQIs during 20000 TTIs for a (randomly chosen) Node B serving 10UEs (none indoor) and a (randomly chosen) HNB serving 1UE. The HNB always transmits at its maximum power (13dBm). Even with such low power, the HUE experiences better transmission quality with high values of reported CQIs (here all values are greater than 15).

When power control (PC) is applied for various $\mathbf{CQI}_{\text{target}}$ values and a monitoring window $L = 5$ (10ms monitoring) under the same conditions, the reported CQIs tend to follow a Gaussian distribution centred around our target as shown in the upper part of Figure 4. There is an exception for $\mathbf{CQI}_{\text{target}} = 22$ which presents a high value at CQI 18, but this value was already frequently reported when no power control was applied (see Figure 3). The higher the target, the harder it becomes for the HUE to report the desired CQI (the increase of the standard deviation is visible), even when transmitting

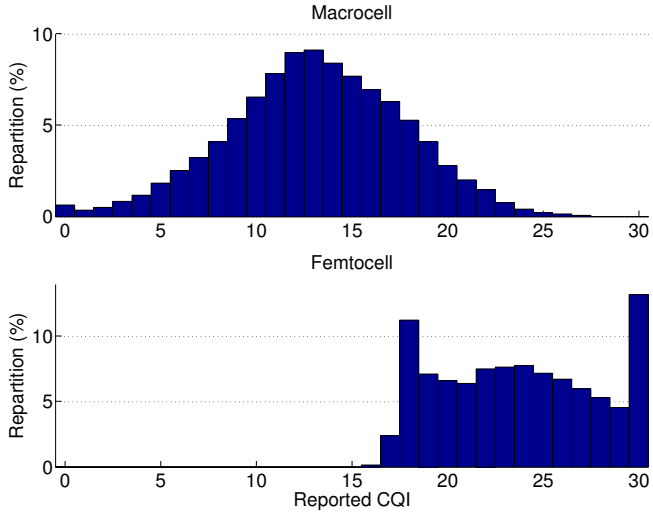

Figure 3: CQI repartition without power control

at maximum power as shown in the lower part of Figure 4 for $\mathbf{CQI}_{\text{target}} = 22$.

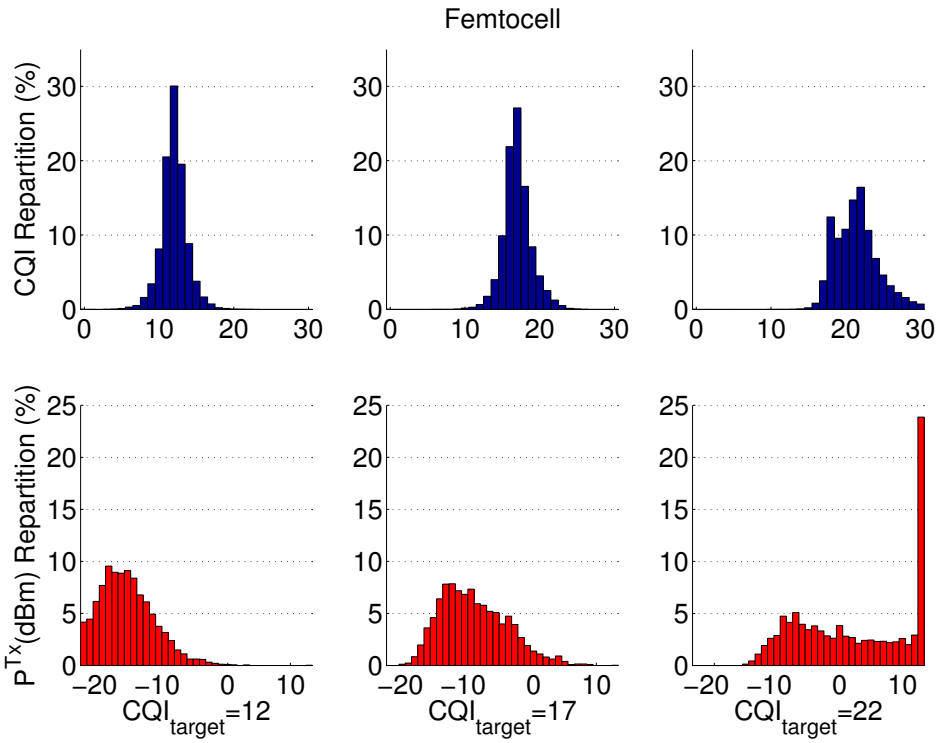

Figure 4: HUE CQI and HNB P^{Tx} repartition with PC ($L = 5$)

The monitoring window length also plays a role in the repartition of the reported CQIs. A smaller length will lead to a greater responsiveness of the algorithm, but the HNB will have less time to adjust its transmit power which gives rise to some hardware constraints. The upper part of Figure 5 shows the reported CQI for different value of L when $\mathbf{CQI}_{\text{target}} = 17$. As expected, a smaller monitoring window allows the HNB to quickly adapt its power: with $L = 2$ (4ms monitoring) the reported CQI is equal to the target during 43% of the time, while with $L = 10$ (20ms monitoring) this value drops

to 17%.

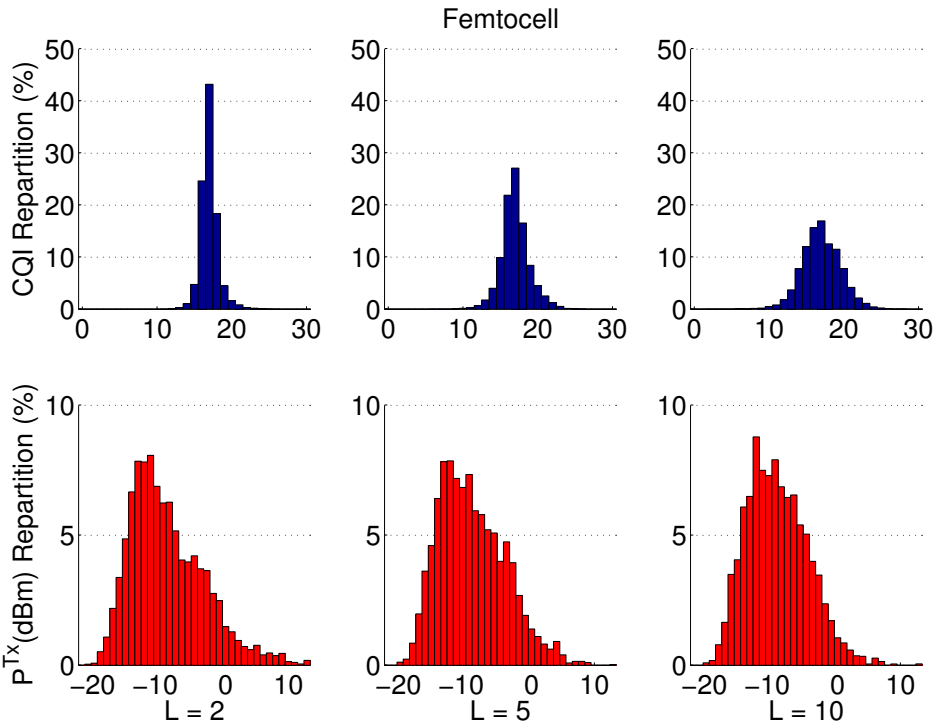

Figure 5: HUE CQI and HNB P^{Tx} repartition with PC ($\text{CQI}_{\text{target}} = 17$)

5.2 System-Level Simulations

As a trade-off between the achievable data rate (should be better than the average macrocell value) and the reactivity of the algorithm, we adopt $\text{CQI}_{\text{target}} = 17$ and $L = 5$ through all the simulations. We collect the throughput of femtocell users and indoor macrocell users (the one that are the most affected by the femtocell deployment) as well as their outage ratio defined as the number of times a UE reports a zero CQI over the total number of its CQI reports. We compare these statistics when the PC algorithm is applied and when the hard approach (HA) defined in 2 is used with the HNB transmitting at its maximum power.

Figure 6 shows that HUEs experience an average throughput of 1.91Mbps and 1.83Mbps for PC and HA, respectively. These values are below the target (CQI=17, i.e. 2.09Mbps), but the CQI is defined with 10% of error probability, equivalent to 1.88Mbps. The HA allows 78% of the HUEs to have a throughput above this latter value, while the PC only allows 40%. In both cases the HUEs experience better transmission than indoor MUEs. If the HA performs better than the PC, it has also a greater impact on the indoor MUEs. The lack of power control leads to an average throughput of 308kbps with 15% of indoor MUEs not being served, while its use allows this value to reach 403kbps (roughly +33% increase) with almost all MUEs being served once (the 5percentile is equal to 7.4kbps).

The benefit of dynamic power control is clearly revealed when the outage ratio is observed in Figure 7. While HUEs reports few outages to their HNB (less than 0.5% of the time), the indoor MUEs are severely impacted by the HNB deployment in closed-access mode. In average, indoor MUEs are 31.5% of the time in outage, thus, not being

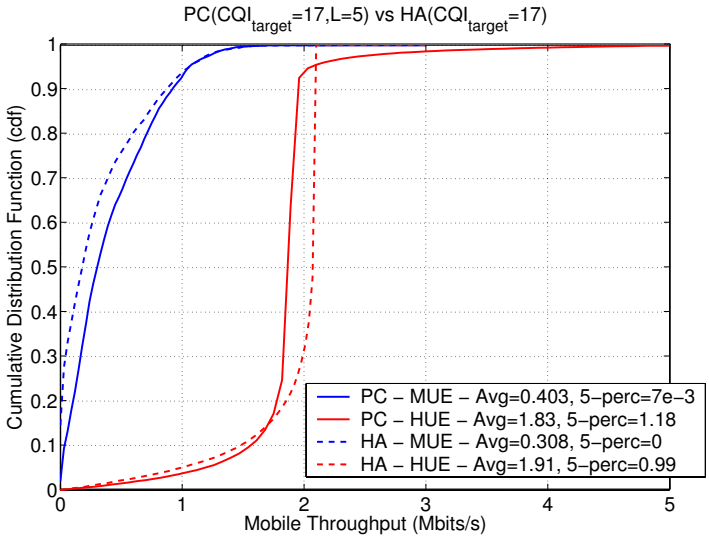

Figure 6: Throughput (Mbps) of indoor MUEs and HUEs

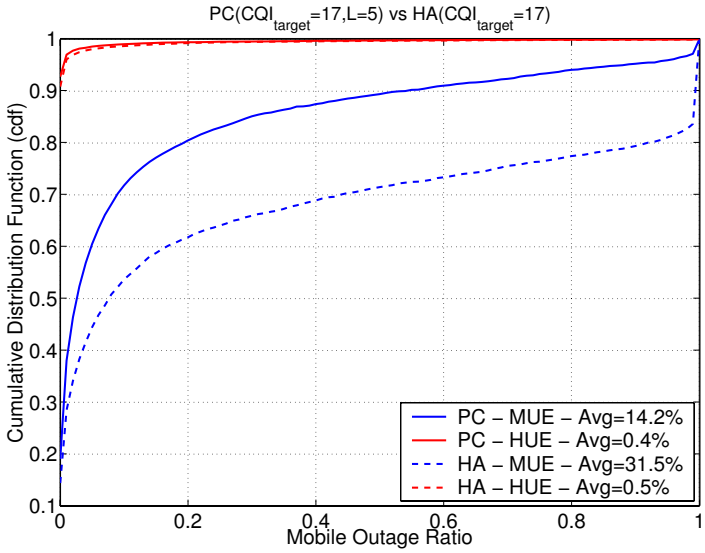

Figure 7: Outage ratio of indoor MUEs and HUEs

able to access the network. With power control this "out-of-service" period is divided by more than 2 (14.2%).

6. Conclusion

We have proposed in this paper a simple and light power control algorithm that can be applied directly at the HNB level. Based on the CQI reporting monitoring, the HNB adjusts on its own its transmission power in order to serve the UE with the appropriate throughput associated to the targeted CQI, whilst keeping transmission reliable enough (maximum 10% error probability). Even though this solution does not perform as well as a direct approach limitating the served MCS to the targeted one, it has an outstanding beneficial impact on the MUEs being in the vicinity of the HNB thanks to a 33% data rate increase and drastic outage reduction by 50%.

Whilst a residential deployment scenario has been our primary focus till now, thus

considering as a reference point a single user case, the rapidly growing interest in corporate environment roll-out will steer our research directions towards simultaneous users assessment in the near future, to complement and refine our current results.

References

[1] Femto Forum, *Interference Management in UMTS Femtocells*, February 2010.

[2] 3GPP, *Overview of Release 8*. 3rd Generation Partnership Project, September 2010.

[3] Global mobile Suppliers Association (GSA), *GSM/3G and LTE Market Update*, March 2011.

[4] Femto Forum, *Interference Management in OFDMA Femtocells*, February 2010.

[5] 3GPP TR 25.967, *FDD Home NodeB RF Requirements*. 3rd Generation Partnership Project, April 2009.

[6] M. Yavuz, F. Meshkati, S. Nanda, A. Pokhariyal, N. Johnson, B. Raghothaman, and A. Richardson, "Interference management and performance analysis of umts/hspa+ femtocells," *IEEE Communications Magazine*, vol. 47, pp. 102–109, September 2009.

[7] R1-104423, *Downlink Power Setting for ICIC in Macro-Femto co-channel Deployment*. 3GPP TSG RAN WG1#62, August 2010.

[8] H. Claussen, L. Ho, and L. Samuel, "Self-optimization of coverage for femtocell deployments," in *Wireless Telecommunications Symposium (WTS 2008)*, pp. 278–285, April 2008.

[9] M. Morita, Y. Matsunaga, and K. Hamabe, "Adaptive power level setting of femtocell base stations for mitigating interference with macrocells," in *IEEE 72nd Vehicular Technology Conference (VTC 2010-Fall)*, pp. 1–5, September 2010.

[10] 3GPP TR 36.921, *FDD Home eNode B (HeNB) Radio Frequency (RF) requirements analysis*. 3rd Generation Partnership Project, March 2010.

[11] 3GPP TS 25.214, *Physical layer procedures (FDD) (Release 9)*. 3rd Generation Partnership Project, December 2010.

[12] R1-020675, *Revised CQI Proposal*. 3GPP TSG RAN WG1#25, April 2002.

[13] 3GPP TR 25.814, *Physical layer aspects for evolved Universal Terrestrial Radio Access (UTRA) (Release 7)*. 3rd Generation Partnership Project, September 2006.

[14] 3GPP TR 36.814, *Further advancements for E-UTRA physical layer aspects (Release 9)*. 3rd Generation Partnership Project, March 2010.

[15] W. Jakes, *Microwave Mobile Communications*. New York: Wiley, 1974.

[16] A. Seeger, M. Sikora, and A. Klein, "Variable orthogonality factor: a simple interface between link and system level simulation for high speed downlink packet access," in *IEEE 58th Vehicular Technology Conference (VTC 2003-Fall)*, vol. 4, pp. 2531–2534, October 2003.

